

Conf-9409314--1

UCRL-JC-118306
PREPRINT

Multidimensional Discretization of Conservation Laws
for Unstructured Polyhedral Grids

Donald E. Burton

This paper was prepared for submittal to the
SAMGOP-94, 2nd International Workshop on Analytical Methods
and Process Optimization in Fluid and Gas Mechanics
VNIIEF, Holiday Base, Arzamas-16, Russia
September 10-16, 1994

August 22, 1994

This is a preprint of a paper intended for publication in a journal or proceedings. Since changes may be made before publication, this preprint is made available with the understanding that it will not be cited or reproduced without the permission of the author.

 Lawrence
Livermore
National
Laboratory

DISTRIBUTION OF THIS DOCUMENT IS UNLIMITED

DISCLAIMER

This document was prepared as an account of work sponsored by an agency of the United States Government. Neither the United States Government nor the University of California nor any of their employees, makes any warranty, express or implied, or assumes any legal liability or responsibility for the accuracy, completeness, or usefulness of any information, apparatus, product, or process disclosed, or represents that its use would not infringe privately owned rights. Reference herein to any specific commercial products, process, or service by trade name, trademark, manufacturer, or otherwise, does not necessarily constitute or imply its endorsement, recommendation, or favoring by the United States Government or the University of California. The views and opinions of authors expressed herein do not necessarily state or reflect those of the United States Government or the University of California, and shall not be used for advertising or product endorsement purposes.

DISCLAIMER

**Portions of this document may be illegible
in electronic image products. Images are
produced from the best available original
document.**

MULTIDIMENSIONAL DISCRETIZATION OF CONSERVATION LAWS FOR UNSTRUCTURED POLYHEDRAL GRIDS

Donald E. Burton
Lawrence Livermore National Laboratory
P.O. Box 808, L-18
Livermore, CA 94550, USA

ABSTRACT

To the extent possible, a discretized system should satisfy the same conservation laws as the physical system. We consider the conservation properties of a staggered-grid Lagrange formulation of the hydrodynamics equations (SGH) which is an extension of a 1D scheme due to von Neumann and Richtmyer (VNR). The term *staggered* refers to spatial centering in which position, velocity, and kinetic energy are centered at nodes, while density, pressure, and internal energy are at cell centers. Traditional SGH formulations consider mass, volume, and momentum conservation, but tend to ignore conservation of total energy, conservation of angular momentum, and requirements for thermodynamic reversibility. We show that, once the mass and momentum discretizations have been specified, discretization for other quantities are dictated by the conservation laws and cannot be independently defined.

Our spatial discretization method employs a *finite volume* procedure that replaces differential operators with surface integrals. The method is appropriate for multidimensional formulations (1D, 2D, 3D) on unstructured grids formed from polygonal (2D) or polyhedral (3D) cells. Conservation equations can then be expressed in *conservation form* in which conserved currents are exchanged between control volumes. In addition to the surface integrals, the conservation equations include source terms derived from physical sources or geometrical considerations.

In Cartesian geometry, mass and momentum are conserved identically. Discussion of volume conservation will be temporarily deferred. We show that the momentum equation leads to a form-preserving definition for kinetic energy and to an exactly conservative evolution equation for internal energy. Similarly, we derive a form-preserving definition and corresponding conservation equation for a zone-centered angular momentum.

In the absence of energy source terms or energy dissipation (such as that produced by artificial

viscosity), difference equations should give rise to no entropy change. That is, the numerical system should be able to reversibly transfer energy back and forth between kinetic and internal reservoirs. Traditional SGH formulations simply postulate an evolution equation for internal energy. Although this might seem sufficient to guarantee reversibility, such is not actually the case because such formulations do not identically conserve energy. We show, however, that our formulation can be made reversible if certain constraints are observed. The first of these requires that volume be defined in terms of a conservation equation instead of the usual direct function of coordinates. The second constraint forbids the use of higher order functional representations for either velocity or stress. That is, stress must be spatially constant within the cell, and velocity, within its control volume. Third, velocity or acceleration interpolation cannot be used.

In addition to the Cartesian form, we present a formulation in 2D axisymmetric geometry, as well as formulations in 1D. In 2D axisymmetric geometry, rotational symmetry of the difference equations must be preserved if spurious on-axis behavior is to be avoided. Generally, rotational symmetry is achieved by replacing the finite volume surface integrals with line integrals. This also causes a deviation from strict conservation form by introducing geometrical terms that appear functionally as sources.

Finally, we discuss artificial viscosity which is used for two purposes: first to introduce the proper entropy change due to shocks and second to reduce spurious oscillations. We also present a 3D generalization of a 2D spurious vorticity damping model that removes both hourglass and chevron instabilities.

MASTER

DISTRIBUTION OF THIS DOCUMENT IS UNLIMITED

1. INTRODUCTION

This paper discusses a Lagrangian hydrodynamics formulation that is multidimensional and is suitable for arbitrarily connected polygonal or polyhedral zones. In this section, we discuss why such a method is of interest, review conservation issues, and describe our notation. The body of the paper presents a multidimensional Cartesian formulation. Formulations in curvilinear geometry are described in the appendices along with several example calculations.

1.1 THE FREE-LAGRANGE METHOD

Problems involving extreme mesh distortions have been traditionally modeled using Eulerian techniques or by Arbitrary Lagrange Euler (ALE) techniques.¹ The free-Lagrange method (FL) offers an alternative that has significant advantages and has been used successfully in 2D for more than 20 years. The term free-Lagrange was first introduced by W.P. Crowley² about 1968, although the earliest work in the area appears to have been done by Pasta and Ulam³ in 1959. Other early work in the US was also done by J. Boris and M. Fritts⁴ and in the USSR by D'yachenko, Glagoleva, Sofronov, and others.⁵

The FL method is characterized by: (a) a Lagrangian hydrodynamics formulation, *i.e.*, mass moves with the mesh thereby minimizing advection error; (b) the use of unstructured grids that permits zoning to be placed where needed with minimal regard to special connectivity rules; and (c) the ability to reconfigure the mesh depending upon the flow.

Several forms of FL have evolved. The most common is limited to triangle/tetrahedral zoning and centers all variables at the mesh points (see for example Trease⁶). A second form⁷ employs a triangular/tetrahedral *dual mesh* constructed by connecting adjacent zone centers. The form described here⁸ employs staggered-grid hydrodynamics (SGH), a generalization of the 1D

von Neumann and Richtmyer (VNR)⁹ scheme known to produce second-order accuracy in the discretized momentum equation. The term *staggered* refers to spatial centering in which position, velocity, and kinetic energy are centered at nodes, while density, pressure, and internal energy are within cells. Generally the SGH discretization is more accurate than tetrahedral methods, especially at interfaces.

It is well known that triangular elements are relatively stiff¹⁰ for continuum mechanics and possibly fluid mechanics applications. Because of this, the 2D SGH form was extended by Crowley⁸ from triangular zones to mixtures of triangles and quadrilaterals. This permitted a strategy of calculating with quadrilateral zones until some deformation criteria is reached, splitting quadrilaterals into triangles where necessary, and later reforming quadrilaterals. One of the eventual goals of the present work is to extend these notions into 3D, resulting in polyhedral not simply tetrahedral zones.

A common approach to discretizing 3D space is to extend the set of permitted elements beyond tetrahedra by adding brick (hexahedra), prism, and pyramid elements. Finite element prescriptions exist for this particular set of elements but not for general polyhedra. This is not a very satisfactory strategy for a FL method because of the need for reconnection. Consider, for example, two adjacent

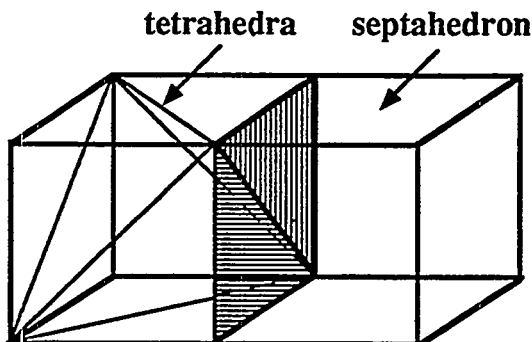


Figure 1. Creation of a septahedron by decomposing one of two adjacent hexahedra into tetrahedra.

brick elements sharing a common quadrilateral face. If one element is tetrahedralized as shown in Figure 1, the joining face must be split into 2 triangles, causing the remaining element to become a septahedron which is not an allowed member of the set.

Consequently, we have chosen an alternative approach that focuses on developing differencing techniques suitable for arbitrary polygons in 2D and polyhedra in 3D. In this way, the numerical differencing is unaffected by the presence of the septahedron in the example. The only spatial discretization paradigm that seems suited to this situation is the *finite volume* method that replaces differential operators with surface integrals. It is appropriate for multidimensional formulations on unstructured grids formed from polygonal (2D) or polyhedral (3D) cells. In particular we excluded from consideration (1) the finite element method which is limited to a relatively small set of polyhedra, and (2) finite difference schemes such as that of Schulz¹¹ because they are restricted to grids which are logically rectangular. We have recently developed data structures and discretization templates that accommodate arbitrary polygonal or polyhedral zoning and are well suited to constructing the finite volume integrals.¹²

1.2 CONSERVATION

The focus of this paper is the investigation of the conservation properties of an SGH formulation of the hydrodynamics equations using a finite volume spatial discretization. To the extent possible, a discretized system should satisfy the same conservation laws as the physical system and should employ *form-preserving* analogs of the physical variables. (A numerical quantity is said to be *form-preserving* when its functional dependence matches that of the physical variable.) Traditional SGH formulations are explicitly constructed to provide mass, volume, and momentum conservation, but tend to only approximate conservation of energy, ignore conservation of angular momentum, and disregard requirements for thermodynamic reversibility. As a consequence of the finite volume discretization,

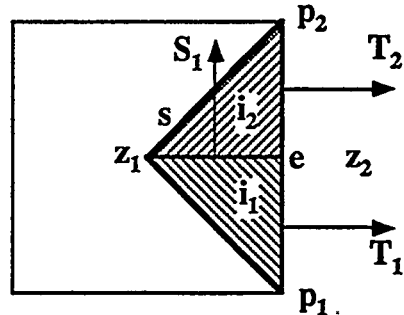


Figure 2. Side template for a rectangular zone.

conservation equations can be expressed in *conservation form* in which conserved currents are exchanged between control volumes.

In Cartesian geometry, mass and momentum are conserved identically. We have previously shown that the momentum equation leads to an exactly conservative evolution equation for internal energy¹³ and to a corresponding conservation equation for a zone-centered angular momentum.¹⁴ We now show that our formulation can be made thermodynamically reversible if certain constraints are observed.

In 2D axisymmetric geometry, we present a form of the difference equations that achieves rotational symmetry by replacing the finite volume surface integrals with line integrals for both momentum and strain. The resulting method is symmetrical, employs an energy-conserving formulation, and avoids the unintended introduction of entropy by the difference equations. However, like other symmetrical formulations, the conservation equations are not in strict conservation form and errors do occur near the axis.

A recurring theme will be that, once the mass and momentum discretizations have been specified, there are very few independent assumptions to be made.

1.3 NOTATION AND CONVENTIONS

For ease of visualization, we will present our derivations in the context of the 2D case, although

the results are valid in 1D and 3D. Further, although most figures will picture quadrilateral zones, the results are valid for arbitrary polygons in 2D and polyhedra in 3D.

Spatial template

For 2D geometry, the zones are divided into triangular areas that will be called *sides* as shown (darkened) in Figure 2 for the special case of a rectangular zone. The *sides* are significant because they are the templates that provide the connectivity between *points*, *zones*, and so forth. The templates are generalizations of those described by Cooper.¹⁵ Each side is divided into two triangular areas called *corners* and labeled *i*.

The analogous 3D *side*¹² is shown in Figure 3. To aid visualization, we have pictured a simple brick zone, but again the scheme works for any polyhedron. Although it may appear that we have introduced very fine detail into the differencing templates, such geometrical detail is necessary because the polyhedral faces are generally non-planar. Each side is further divided into two tetrahedral *corner* volumes labeled *i*.

Figures 2 and 3 also show the surface area vectors S_i and T_i that are fundamental in defining finite volume surface integrals.

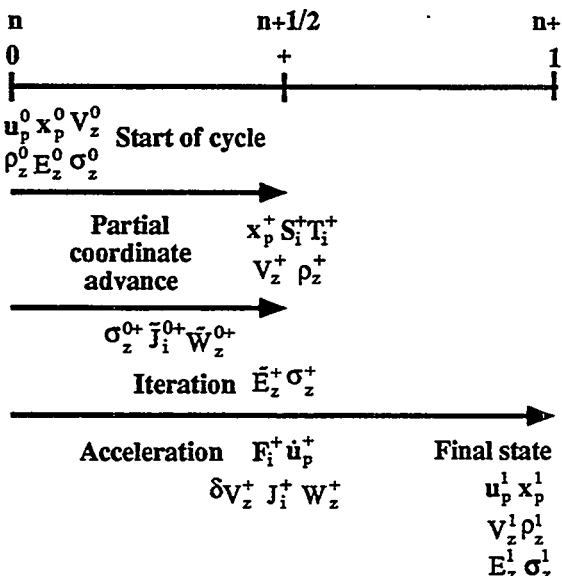


Figure 4. Time centering of variables.

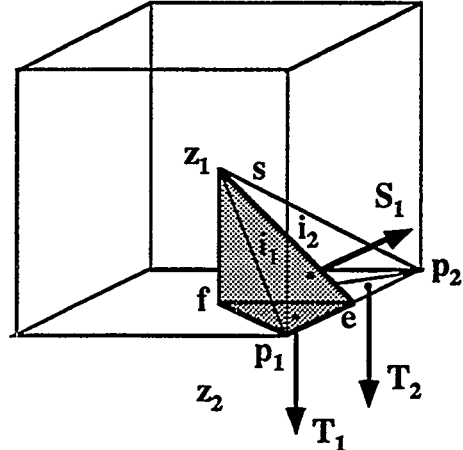


Figure 3. Side template for a hexahedral zone. S_1 is normal to plane efz_1 and T_1 is normal to plane $fepl_1$.

Indices are used to point to memory locations in which data, such as physical coordinates, might be stored. The *p* index refers to points that define the mesh. To form numerical integrals, other auxiliary points are also needed corresponding to zone (*z*), edge (*e*), and face (*f*) centers. The coordinates of these points are derived from the points *p*. A surprising result of this work will be that the physical location of the point coordinates are relatively unimportant to the differencing, while the differencing is sensitive to the *e* and *f* points.

For each corner index *i* there is an implied set of indices $\{p, z, e, f, s\}$, and for each side index *s* there is an implied set of primary indices $\{p1, p2, z, f\}$ and an auxiliary set $\{i1, i2, z2, e\}$.

Time Centering

Unlike the original VNR scheme which was also temporally staggered, our method uses a temporal centering, termed *even-time*, in which most final-state variables are centered at the full timestep. The simultaneous advancement of both position and internal energy requires a logically implicit calculation that is approximated using a predictor-corrector procedure to calculate a half-timestep acceleration used for advancing velocity.

The time-centering of the variables is shown in Figure 4 for purposes of establishing notation. The exact definitions of the variables will be discussed

later. We use the superscript notation {-, 0, +, 1} to indicate time centering of {n-1/2, n, n+1/2, and n+1} respectively. Subscripts refer to spatial centering.

Capitalized quantities are extensive while lower cased quantities are intensive or specific.

2. CARTESIAN GEOMETRY

This section presents a multidimensional hydrodynamics formulation in Cartesian geometry. Curvilinear formulations are given in Appendix A. Rather than simply postulating the entire formulation at the outset, we will begin with minimal initial postulates, and add to them as more are required.

2.1 MASS CONSERVATION

Since we consider only a Lagrangian formulation, we postulate that the mass in each corner volume is constant.

$$M_i = \text{constant} \quad 2.1.1$$

$$M_z = \sum_i^z M_i \quad 2.1.2$$

$$M_p = \sum_i^p M_i \quad 2.1.3$$

where the notation \sum_i^p and \sum_i^z refer to sums over corners i surrounding respectively a point p or a zone z .

In practice, the zone mass is first computed from the specified initial density ρ_z^{00} and volume V_z^{00} ,

$$M_z = \rho_z^{00} V_z^{00} \quad 2.1.4$$

and the resulting mass is partitioned to M_i based upon a mass fraction φ_i

$$M_i = \varphi_i M_z \quad 2.1.5$$

The fractions φ_i can be defined in several ways. Our experience to date has been that best numerical results are obtained from a surface area weighting

$$\varphi_i = \frac{|\mathbf{T}_i \cdot \hat{\mathbf{x}}_{pz}|}{\sum_i^z |\mathbf{T}_i \cdot \hat{\mathbf{x}}_{pz}|} \quad 2.1.6a$$

where $\hat{\mathbf{x}}_{pz}$ is a unit vector from the zone center to the respective point and \mathbf{T}_i is a zone surface vector. Equal mass weighting also produced satisfactory results (n_z being the number of corners in the zone).

$$\varphi_i = 1/n_z \quad 2.1.6b$$

True area/volume weighting produced the poorest results.

$$\varphi_i = V_i^{00} / V_z^{00} \quad 2.1.6c$$

2.2 MOMENTUM CONSERVATION

Forces

As shown in Figure 5, each point p is surrounded by surfaces that define the *momentum control volume*. Forces result from *reversible* and *irreversible* stress fields σ and π that exist within the zone or side. The stress on each element of surface S_i of the momentum control volume results in forces R_i due to reversible fields and Q_i due to the irreversible fields. We will show in a later section that the reversible stress fields must be centered at the zone, but will not at this point restrict the notation to reflect this. Sign conventions are such that the pressure is given by (summing over repeated indices)

$$P = -\sigma_{ii}/3 \quad 2.2.1$$

Since stress at + depends upon energy while energy is incremented from 0 to + by the $P\delta v$ work, the two must be solved for simultaneously. This can be done

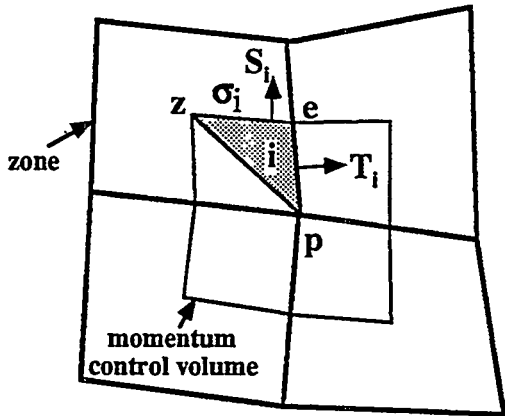


Figure 5. Zone and momentum control volumes, showing surface vectors.

in many ways, and we simply note that we use a predictor-corrector iteration.

Then let us assume that the stresses are known, and we can calculate forces \mathbf{F}_i^+ time centered at $n+1/2$ on the surfaces S_i

$$\mathbf{F}_i^+ = \mathbf{R}_i^+ + \mathbf{Q}_i^+ \quad 2.2.2$$

$$\begin{aligned} \mathbf{R}_i^+ &= \mathbf{S}_i^+ \cdot \boldsymbol{\sigma}_i^+ \\ \mathbf{Q}_i^+ &= \mathbf{S}_i^+ \cdot \boldsymbol{\pi}_i^+ \end{aligned} \quad 2.2.3$$

so that the total force on point p is

$$\mathbf{F}_p^+ = \sum_i^p \mathbf{F}_i^+ \quad 2.2.4$$

Conservation requires that the forces sum to zero on the boundary of the momentum control volume (Newton's third law); that is,

$$\mathbf{F}_{i_1}^+ = -\mathbf{F}_{i_2}^+ \quad 2.2.5$$

Since

$$\mathbf{S}_{i_1}^+ = -\mathbf{S}_{i_2}^+ \quad 2.2.6$$

the finite volume method automatically accomplishes this providing

$$\begin{aligned} \boldsymbol{\sigma}_{i_1}^+ &= \boldsymbol{\sigma}_{i_2}^+ \\ \boldsymbol{\pi}_{i_1}^+ &= \boldsymbol{\pi}_{i_2}^+ \end{aligned} \quad 2.2.7$$

at the surface.

Acceleration and Velocity

The control volume plays the role of an accounting device in which the conserved momentum of the system can always be accumulated. The force at $+$ imparts an acceleration to the momentum control volume, presumably to the center of mass. Later, we will show that we must take this acceleration to be constant throughout the volume, although we do not explicitly make this assumption at this point. The acceleration is calculated from

$$M_p \dot{\mathbf{u}}_p^+ = \mathbf{F}_p^+ \quad 2.2.8$$

Velocity is integrated using a central difference scheme

$$\mathbf{u}_p^1 = \mathbf{u}_p^0 + \dot{\mathbf{u}}_p^+ \delta t^+ \quad 2.2.9$$

The value at $+$ is not arbitrary, but is chosen for consistency with kinetic energy equations to be described below.

$$\mathbf{u}_p^+ \equiv \frac{1}{2} (\mathbf{u}_p^0 + \mathbf{u}_p^1) \quad 2.2.10$$

The coordinate integration will also be described later.

2.3 ENERGY

Kinetic Energy

Trulio and Trigger¹⁶ pointed out in 1961 that the VNR method was not energy-conserving and proposed conservative methods for the one-dimensional equations. Their 1D formulation retained the spatial staggering of VNR but relinquished the temporal staggering. Burton¹³ derived a temporally staggered form for unstructured multidimensional grids. The following derivation is for an even-time scheme. By considering the momentum equations in the half intervals $[0, +]$ and $[+, 1]$ and dotting them into the respective velocities at 0 and 1, the evolution equation for kinetic energy is derived

$$\begin{aligned}
K_p^+ - K_p^0 &= \frac{M_p}{2} (u_p^1 - u_p^0) \cdot u_p^0 \\
&= \frac{\delta t^+}{2} F_p^+ \cdot u_p^0 \\
&= \sum_i^p J_i^{0+}
\end{aligned} \tag{2.3.1}$$

$$\begin{aligned}
K_p^1 - K_p^+ &= \frac{M_p}{2} (u_p^1 - u_p^0) \cdot u_p^1 \\
&= \frac{\delta t^+}{2} F_p^+ \cdot u_p^1 \\
&= \sum_i^p J_i^{+1}
\end{aligned} \tag{2.3.2}$$

where we have identified the following form preserving definitions of kinetic energy

$$\begin{aligned}
K_p^0 &\equiv \frac{M_p}{2} u_p^0 \cdot u_p^0 \\
K_p^+ &\equiv \frac{M_p}{2} u_p^1 \cdot u_p^0
\end{aligned} \tag{2.3.3}$$

The latter corresponds to a definition originally made by Trulio and Trigger. We also identified energy currents J between the zone and the point arising from forces on the surface S_i

$$\begin{aligned}
J_i^{0+} &\equiv \frac{\delta t^+}{2} F_i^+ \cdot u_p^0 \\
J_i^{+1} &\equiv \frac{\delta t^+}{2} F_i^+ \cdot u_p^1
\end{aligned} \tag{2.3.4}$$

Then in the full interval $[0, 1]$, the kinetic energy of a point changes by

$$\begin{aligned}
K_p^1 - K_p^0 &= (K_p^+ - K_p^0) + (K_p^1 - K_p^+) \\
&= \frac{\delta t^+}{2} F_p^+ \cdot (u_p^0 + u_p^1) \\
&= \sum_i^p J_i^+
\end{aligned} \tag{2.3.5}$$

where

$$\begin{aligned}
J_i^+ &\equiv J_i^{0+} + J_i^{+1} \\
&= \delta t^+ F_i^+ \cdot u_p^+
\end{aligned}$$

Work and Internal Energy

The discrete SGH system has only two energy reservoirs, internal in the zone and kinetic at the node. The zone is viewed as a system without explicitly modeled kinetic energy but with a velocity

boundary condition. Similarly, the node is a system having only kinetic energy. Thus, the work done by a zone on the surrounding nodes is simply the sum of the exiting energy currents about the zone

$$\begin{aligned}
W_z^+ &= \sum_i^z J_i^+ \\
&= \delta t^+ \sum_i^z F_i^+ \cdot u_p^+
\end{aligned} \tag{2.3.6}$$

Most SGH hydrodynamics formulations simply assert that the work is $P\delta V$ where δV is defined to be a time difference of volumes that are functions of coordinates $V_z = V(x_p)$. Such formulations, which we will denote as PDV, do not exactly conserve energy. As will be discussed shortly, our work expression, which does conserve energy, does not reduce to this particular definition. Implications of this will be discussed below.

Energy is exchanged through the boundary via heat transfer δH and work W . The zonal energy balance is then

$$\begin{aligned}
\delta E_z^+ &= \delta H_z^+ - W_z^+ \\
&= \delta H_z^+ - \sum_i^z J_i^+
\end{aligned} \tag{2.3.7}$$

Entropy and Reversibility

The work can be resolved into parts W_r resulting from reversible forces R and W_q due to irreversible viscous or plastic forces Q . The energy balance for the zone can then be written

$$\begin{aligned}
\delta E &= T\delta S - W_r \\
&= (\delta H - W_q) - W_r
\end{aligned} \tag{2.3.8}$$

We require that all viscous or plasticity models be dissipative, *i.e.*,

$$W_q = \delta t^+ \sum_i^z Q_i^+ \cdot u_p^+ \leq 0 \tag{2.3.9}$$

so that the second law of thermodynamics is satisfied

$$T\delta S = \delta H - W_q \geq \delta H \tag{2.3.10}$$

In the absence of heating or viscous forces, reversibility implies that energy can be converted between kinetic and internal reservoirs via the momentum equation without loss. *Because energy is not exactly conserved in PDV formulations, they cannot satisfy the reversibility condition.* However, our numerical expression for the change in internal energy seems to guarantee that no entropy is produced under these conditions. That is, the energy change for the zone involves only reversible fields and is exactly given by

$$\begin{aligned}\delta E_z^+ &\rightarrow -\delta t^+ \sum_i^z R_i^+ \cdot u_p^+ \\ &= -\delta t^+ \sum_i^z S_i^+ \cdot \sigma_i^+ \cdot u_p^+ \\ &= -W_r\end{aligned}\quad 2.3.11$$

so that if we were to explicitly integrate a *numerical entropy* \hat{S} , it would properly not change under these conditions, *i.e.*,

$$T\delta\hat{S} = \delta E + W_r = 0 \quad 2.3.12$$

However, this is not the complete picture because such a numerical entropy is not explicitly used except perhaps as a calculational diagnostic. That is, this numerical entropy is fictitious, and the true entropy is that which comes from the equation of state (EOS).

The *entropy* S is not an independently integrable quantity, but is rather a dependent variable of the EOS which has specific volume and energy as independent variables. Therefore, the actual entropy change comes from an iterative calculation of the form

$$\begin{aligned}\delta S &= EOS(E^1, V^1) - S^0 \\ &= EOS(E^0 + \delta E, V^0 + \delta V) - S^0\end{aligned}\quad 2.3.13$$

Because this is not an algebraically exact calculation, there will always be accuracy issues associated with large steps or incomplete convergence. We are not concerned with this type of error which is controllable, but rather with a more serious potential error associated with the form of δE .

For simplicity consider an adiabatic gas system. For points sufficiently near each other, the EOS was explicitly constructed to satisfy $\delta E = -P\delta V$ along an adiabat. In the traditional PDV formulation, δE is simply set to $-P\delta V$, so that δV and δE are consistent with the EOS, although not conservative.

However, in our formulation, δE is fixed by the energy conserving formulation, and we have not as yet defined δV . If we make no attempt to guarantee exact consistency of the two, our numerical model will generally yield $\delta E \neq -P\delta V$ even though no viscous forces are present. *Failure of the differencing scheme to satisfy such a consistency relationship will appear as unintended entropy errors (deviations from the adiabat).* The solution, of course, is to define a consistent δV which is done in a later section.

Constraint on the stress field

It follows from the preceding discussion that the form of the strain or volume calculation cannot be arbitrarily chosen, but is in fact dictated by the initial discretization chosen for the momentum equation. That is, it must be defined such that the following is true for a fluid

$$\begin{aligned}W_z^+ &= -\delta t^+ \sum_i^z P_i^+ S_i^+ \cdot u_p^+ \\ &\rightarrow P_z^+ \delta V_z^+\end{aligned}\quad 2.3.14$$

The first step in establishing the desired relationship is to factor the zonal pressure P_z from the sum. This can only be done if $P_i = P_z$. Consequently, extensions to SGH with side-centered stresses such the TTS¹⁷ method cannot be exactly reversible. We are then constrained to use only a so called *constant stress element*, resulting in

$$W_z^+ = P_z^+ \left\{ -\delta t^+ \sum_i^z S_i^+ \cdot u_p^+ \right\} \quad 2.3.15$$

This particular argument does not apply to the viscous forces Q which are intended to be dissipative and do not need to be factored from the corresponding sum.

For a solid, the corresponding work equation need to be

$$\begin{aligned} W_z^+ &= \delta t^+ \sum_i^z S_i^+ \cdot \sigma_i^+ \cdot u_p^+ \\ &= -\sigma_z^+ : \left\{ -\delta t^+ \sum_i^z S_i^+ u_p^+ \right\} \\ &\rightarrow -\sigma_z^+ : \delta D_z^+ \end{aligned} \quad 2.3.16$$

where : denotes contraction on both indices, and

$$\delta D_z^+ = \delta t^+ V_z^+ \nabla u \quad 2.3.17$$

is a deformation tensor and includes dilatational, shear, and rotational components. In the next section, we establish that the above correspond to reasonable discretizations for δV and δD ; *i.e.*,

$$\begin{aligned} \delta V_z^+ &= -\delta t^+ \sum_i^z S_i^+ \cdot u_p^+ \\ \delta D_z^+ &= -\delta t^+ \sum_i^z S_i^+ u_p^+ \end{aligned} \quad 2.3.18$$

2.4 VOLUME AND STRAIN

Obviously, we cannot simply postulate that $V=V(x)$. Instead, we propose an evolution equation for volume in conservation form and will verify that it is equivalent to Equation 2.3.18

$$\begin{aligned} \delta V_z^+ &= \delta t^+ V_z^+ (\nabla \cdot u) \\ &= \delta t^+ \oint_z dT \cdot u \\ &\rightarrow \delta t^+ \sum_i^z T_i^+ \cdot u_p^+ \end{aligned} \quad 2.4.1$$

Note that volume is rigorously conserved even though it may not be exactly what might be calculated directly from the coordinates. This is easily shown to reduce to the form required by the reversibility constraint. We rely upon the fact that the velocity u_p is constant within the momentum control volume and that $S_1 + S_2 = -(T_1 + T_2)$ as shown in Figure 6. This is simply a statement of the path independence of the integral between e_1 and e_2 providing σ_z and u_p are constant along the path. The same result obtains in 3D. As was the case with

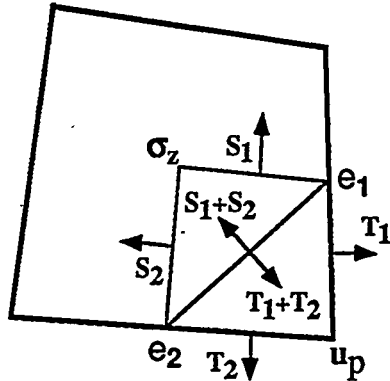


Figure 6. Path independence of the volume integral.

stress, use of a higher order spatial dependence for u_p would destroy the path independence of the integral. In particular, velocity or acceleration interpolation cannot be used, such as has been suggested to correct for the center-of-mass of the momentum control volume.^{18,19} Our point is that such extensions to SGH are unintentionally dissipative, not that they fail to serve useful purposes or should not be employed.

Then we have shown that the volume change can be written as in Equation 2.3.18

$$\delta V_z^+ = -\delta t^+ \sum_i^z S_i^+ \cdot u_p^+ \quad 2.4.2$$

and the corresponding deformation equation as

$$\begin{aligned} \delta D_z^+ &= \delta t^+ V_z^+ \nabla u \\ &= \delta t^+ \oint_z dT \cdot u \\ &\rightarrow \delta t^+ \sum_i^z T_i^+ u_p^+ \\ &= -\delta t^+ \sum_i^z S_i^+ u_p^+ \end{aligned} \quad 2.4.3$$

Another convenient form for these equations is

$$\begin{aligned} \delta V_z^+ &= -\delta t^+ \sum_s^z S_s^+ \cdot (u_{p1}^+ - u_{p2}^+) \\ \delta D_z^+ &= -\delta t^+ \sum_s^z S_s^+ (u_{p1}^+ - u_{p2}^+) \end{aligned} \quad 2.4.4$$

where $S_s^+ \equiv S_{i_s}^+$. This is useful in defining artificial viscosity tensors.

The zone specific volume used in EOS calculations is given by

$$v_z = \frac{V_z}{M_z}$$

$$V_z = V_z^{00} + \sum_n \delta V_z^+$$

2.4.5

2.5 COORDINATES

After substituting a conservative integral for the explicit volume expression, examination of the difference equations reveals an extremely significant fact. The momentum contained in the control volume about a point remains important as the primary momentum accounting device, but the specific point coordinates x_p do not play a role in the differencing. What actually matters are the coordinates of the edge centers x_e (and face centers x_f in 3D) that are advanced using a momentum conserving average of adjacent point velocities given by

$$\begin{aligned} u_e^+ &= \frac{1}{M_e} \sum_i^e M_i u_p^+ \\ u_f^+ &= \frac{1}{M_f} \sum_i^f M_i u_p^+ \\ u_z^+ &= \frac{1}{M_z} \sum_i^z M_i u_p^+ \end{aligned} \quad 2.5.1$$

with similar expressions at times 0 and 1. In order to mechanically form the surface S_i vectors, control points x_z and x_p are needed in addition to x_e and x_f , but mathematically drop out of the integrals. The coordinates for the auxiliary points can be directly integrated. However, since we use constant mass weights, a more economical alternative procedure for calculating the auxiliary points is possible. If the point velocity is formally integrated

$$\begin{aligned} x_p^+ &= x_p^0 + \frac{\delta t^+}{2} u_p^0 \\ x_p^1 &= x_p^+ + \frac{\delta t^+}{2} u_p^1 \\ &= x_p^0 + \delta t^+ u_p^+ \end{aligned} \quad 2.5.2$$

then the auxiliary coordinates can be found using the same weighted averages as in the velocity equations

$$x_e^+ = \frac{1}{M_e} \sum_i^e M_i x_p^+ \quad 2.5.3$$

with similar expressions for x_f and x_z .

Hourglass instability and coordinates

It is also well known that SGH suffers from spurious modes on the scale of the mesh size because of degrees of freedom unconstrained by the difference equations. One such mode is the *hourglass* mode shown in Figure 7. By definition, an hourglass mode is any mode of deformation that does not change the zone volume or strain and therefore produces no response from the constitutive model. There exist many *ad hoc* artificial viscosity schemes successful in reducing hourglass distortion without affecting physical *shear* modes. The smoothing viscosities discussed in a later section are effective against instabilities such as hourgassing.

However, unless we introduce special artificial viscosities that are themselves sensitive to hourgassing, the only manifestation of the spurious mode is through the point coordinates x_p . But, as we have shown, the specific point coordinates do not play a role in the differencing either. It follows that the major consequence of hourglass modes is simply that the grid may appear distorted, not that the quality of the solution has been compromised. We are justified therefore in independently moving the points, without adjusting velocity, anywhere aesthetics demands. There is not even a requirement that edges formed from pairs of points be straight lines. We propose advancing the point using the center-of-mass velocity of the surrounding zones

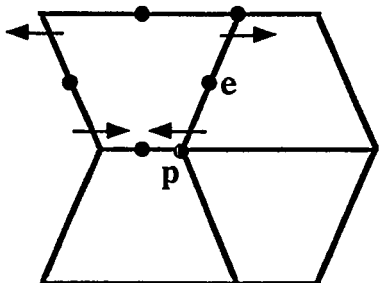


Figure 7. Typical hourglass instability.

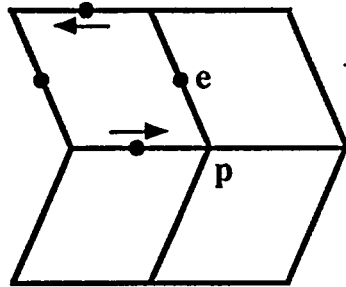


Figure 9. Example of chevron instability.

$$\begin{aligned}
 \mathbf{U}_p &= \frac{1}{M_p} \sum_i^p M_i \mathbf{u}_z \\
 \mathbf{X}_p^+ &= \mathbf{X}_p^0 + \frac{\delta t^+}{2} \mathbf{U}_p^0 \\
 \mathbf{X}_p^1 &= \mathbf{X}_p^+ + \frac{\delta t^+}{2} \mathbf{U}_p^1 \\
 &= \mathbf{X}_p^0 + \delta t^+ \mathbf{U}_p^+
 \end{aligned} \tag{2.5.4}$$

As a practical matter, these results do not eliminate from concern other instabilities such as *chevron* modes which occur in fluids because the constitutive model does not respond to shear deformation. Further, although pure hourglass modes do not themselves degrade the solution, they are seldom pure. That is, velocity patterns that appear in one zone as hourgassing typically show up in an adjacent one as a chevron or other mode.

2.6 ARTIFICIAL VISCOSITY

Artificial viscosity serves two principal functions: first to attain the correct shock dissipation, and second to smooth numerical noise. In this section, we consider both functions and also two spatial centerings of the viscosity tensor, zone-centered and side-centered. The requirement that the viscous work be dissipative $W_q \leq 0$ greatly constrains the permissible form of artificial viscosity equations.

Zone-centered viscosity

Consider the case of a zone-centered viscosity tensor. The viscous work equation reduces to

$$\begin{aligned}
 W_q &= \delta t^+ \sum_i^z Q_i^+ \cdot \mathbf{u}_p^+ \\
 &= \delta t^+ \sum_i^z \pi_i^+ : S_i^+ \mathbf{u}_p^+ \\
 &= \delta t^+ \pi_z^+ : \sum_i^z S_i^+ \mathbf{u}_p^+ \\
 &= -\pi_z^+ : \delta D_z^+
 \end{aligned} \tag{2.6.1}$$

so that we can guarantee dissipation if we choose

$$\pi_z^+ \propto (\delta D_z^+)^T \propto \nabla^T \mathbf{u}$$

The velocity gradient can be decomposed into strain and rotational rate tensors

$$\begin{aligned}
 \nabla \mathbf{u} &= \boldsymbol{\varepsilon} + \boldsymbol{\omega} \\
 \boldsymbol{\omega} &= \frac{1}{2} (\nabla \mathbf{u} - \nabla^T \mathbf{u})
 \end{aligned} \tag{2.6.2}$$

The usual approach in defining a viscosity tensor would be to discard the rotational component, arguing that rotations should not be damped. However, the *chevron* instability (illustrated in Figure 9) which occurs in fluids and low-strength solids is an example of a spurious rotational numerical mode that also requires filtering.

Let us first consider shocks. On the scale of an individual zone, shocks are physically planar so that the viscous forces should only be parallel to the direction of propagation \hat{c} . This means that we must eliminate non-shock components of $\nabla \mathbf{u}$ such as those which might arise from convergent flow. The direction of propagation \hat{c} can be found in a number of ways, such as by diagonalizing the strain rate tensor $\boldsymbol{\varepsilon}$. The viscosity tensor can then be written

$$\pi_z^+ = -\rho_z f L_z \tilde{\boldsymbol{\varepsilon}} \tag{2.6.3}$$

where the effective strain rate tensor is obtained by removing the non-shock components

$$\begin{aligned}
 \tilde{\boldsymbol{\varepsilon}} &= (\boldsymbol{\varepsilon} : \hat{c} \hat{c}) \hat{c} \hat{c} \\
 f &= (q_2 |\Delta \mathbf{u}| + q_1 c) \Theta(\Delta \mathbf{u}) \\
 \Delta \mathbf{u} &= L_z \tilde{\boldsymbol{\varepsilon}} : \hat{c} \hat{c} \\
 \Theta(\Delta \mathbf{u}) &= \begin{cases} 1 & \text{compression} \\ 0 & \text{expansion} \end{cases}
 \end{aligned} \tag{2.6.4}$$

L_z is the zone width in the direction of propagation \hat{c} , c is the soundspeed, and ρ_z is the zone density. The quantities q_1 and q_2 are multipliers for the linear and quadratic viscosities. For a γ -law gas typically recommended values follow from analytical shock solutions²⁰

$$\begin{aligned} q_1 &= 0.1 \\ q_2 &= \frac{1}{2}(\gamma+1) \end{aligned}$$

The net effect of this form is to produce a force on each surface parallel to the direction of propagation

$$\begin{aligned} Q_s &= S_s \cdot \pi_s^+ \\ &\propto (S_s \cdot \hat{c})(\varepsilon : \hat{c}\hat{c})\hat{c} \end{aligned} \quad 2.6.5$$

Next, let us consider viscosity used for smoothing. The linear q is an example of such a viscosity with a serious flaw. If problems are calculated long enough, the linear q could, in principle, smooth until all velocity gradients have disappeared. For this reason, it is preferable to avoid linear q and use an alternative

$$\pi_z^+ \propto -\rho_z c L (\nabla u - \bar{\nabla} u)^T \quad 2.6.6$$

in which L is a characteristic length and $\bar{\nabla} u$ is an average velocity gradient which has been spatially smoothed in some fashion. This form causes the velocity gradient to relax toward the local average, as opposed to the value of zero used in the linear q . In practice, the velocity gradient is separated into volumetric θ , deviatoric λ , and rotational ω tensors, and different multipliers are permitted on each

$$\begin{aligned} \nabla u - \bar{\nabla} u &\rightarrow q_v(\theta - \bar{\theta}) \\ &+ q_d(\lambda - \bar{\lambda}) \\ &+ q_w(\omega - \bar{\omega}) \end{aligned} \quad 2.6.7$$

This form has not been proved to be rigorously dissipative, but this has not been a problem in practice.

Side-centered viscosity

An alternative to the zone-centered viscosity is one centered on the side. The viscous work reduces to

$$\begin{aligned} W_q &= \delta t^+ \sum_i^z Q_i^+ \cdot u_p^+ \\ &= \delta t^+ \sum_i^z \pi_s^+ : S_i^+ u_p^+ \\ &= \delta t^+ \sum_s \pi_s^+ : S_s^+ u_{12} \end{aligned} \quad 2.6.8$$

where

$$u_{12} \equiv u_{p_1}^+ - u_{p_2}^+ \quad 2.6.9$$

We can guarantee dissipation if we choose

$$\begin{aligned} \pi_s^+ &= -\rho_z f \hat{S}_s^+ |\hat{u}_{12} \cdot \hat{c}| u_{12} \\ Q_s^+ &= S_s^+ \cdot \pi_s^+ \\ &= -\rho_z f S_s^+ \cdot \hat{S}_s^+ |\hat{u}_{12} \cdot \hat{c}| u_{12} \\ &= -\rho_z f |S_s| |\hat{u}_{12} \cdot \hat{c}| u_{12} \end{aligned} \quad 2.6.10$$

where

$$f = (q_2 |u_{12}| + q_1 c) \Theta(u_{12}) \quad 2.6.11$$

The restoring force on each side is proportional to the velocity difference u_{12} between the two points. The *ad hoc* factor $|\hat{u}_{12} \cdot \hat{c}|$ has been introduced to eliminate non-shock components of u_{12} such as those which might arise from convergent flow.

A variation on a form due to Barton²¹

$$\begin{aligned} \pi_s^+ &= -\rho_z f |\hat{u}_{12} \cdot \hat{c}| \hat{u}_{12} u_{12} \\ Q_s^+ &= S_s^+ \cdot \pi_s^+ \\ &\rightarrow -\rho_z f |S_s \cdot \hat{u}_{12}| |\hat{u}_{12} \cdot \hat{c}| u_{12} \end{aligned} \quad 2.6.12$$

also produces a restoring force proportional to the velocity difference u_{12} and is rigorously dissipative. The absolute value of the dot product $S_s \cdot \hat{u}_{12}$ has been taken to avoid pathological attractive forces which could otherwise occur.

Yet another variation comes from calculating a gradient $\nabla_s u$ from the motion of the side points $\{p1, p2, z, f\}$

$$\begin{aligned}\pi_s^+ &\propto -\rho_z f |x_{12}| \nabla_s u^T \\ Q_s^+ &= S_s^+ \bullet \pi_s^+\end{aligned}\quad 2.6.13$$

which produces a resulting force that is not necessarily parallel to u_{12} , so that dissipation is not guaranteed but has not been a problem in practice. This form (and the next) can be made rigorously dissipative by retaining only the component of the gradient parallel to u_{12}

$$\nabla_s u \rightarrow [\nabla_s u : \hat{u}_{12} \hat{u}_{12}] \hat{u}_{12} \hat{u}_{12}$$

We have not fully investigated the consequences of this variation.

A variation of the previous form is a side-centered viscosity used only for purposes of smoothing

$$\begin{aligned}\pi_s^+ &\propto -\rho_z c |x_{12}| (\nabla_s u - \bar{\nabla}_s u)^T \\ Q_s^+ &= S_s^+ \bullet \pi_s^+\end{aligned}\quad 2.6.14$$

Again dissipation is not guaranteed. This form is a multidimensional generalization of the spurious-vorticity-damping method (SVD)¹⁴ and is effective against both chevron and hourglass instability (see Figures 7 and 9).

2.7 ANGULAR MOMENTUM

Unlike kinetic energy which directly enters the differencing through the internal energy, the numerical angular momentum appears only as a diagnostic. However, the analysis is important for understanding the source of common SGH instabilities and for establishing that the zone center is free of such instabilities.

Let us briefly review the kinematics of angular momentum and the role of the center of mass (CM). For a system of particles satisfying Newton's law, the rate of change of angular momentum is equal to the total applied torque. For any point r , this balance

equation can be separated as follows into rates associated with the point and about the point.

$$\sum_i m_i r_i \times \dot{u}_i = \sum_i r_i \times f_i \quad 2.7.1$$

$$Mr \times \dot{U} + \sum_i m_i (r_i - r) \times \dot{u}_i = r \times F + \sum_i (r_i - r) \times f_i \quad 2.7.2$$

$$\dot{L}(r) + \lambda(r) = T(r) + \tau(r) \quad 2.7.3$$

where

$$M \equiv \sum_i m_i \quad F \equiv \sum_i f_i \quad 2.7.4$$

$$T(r) \equiv r \times F \quad \tau(r) \equiv \sum_i (r_i - r) \times f_i$$

$$R \equiv \frac{1}{M} \sum_i m_i r_i \quad U \equiv \frac{1}{M} \sum_i m_i u_i = \dot{R}$$

$$\dot{L}(r) \equiv Mr \times \dot{U} \quad \lambda(r) \equiv \sum_i m_i (r_i - r) \times \dot{u}_i$$

However, only for the CM point $r = R$ is the integral of \dot{L} a constant of the motion, so that

$$\begin{aligned}L(R) &\equiv \int dt MR \times \dot{U} \\ &= \int dt M(R \times \dot{U} + \dot{R} \times U) \\ &= \int dt \frac{d}{dt} MR \times U \\ &= MR \times U\end{aligned}\quad 2.7.5$$

For this particular reference point, the angular momentum of the point and the intrinsic angular momentum about the point can be independently integrated

$$\begin{aligned}\dot{L}(R) &= T(R) \\ \lambda(R) &= \tau(R)\end{aligned}\quad 2.7.6$$

We must show that the former conservation equation for angular momentum is satisfied by our numerical system. To do this we must (a) establish a center of mass, (b) define a control volume, and (c)

express the torque on the right hand side as a sum of fluxes across the control volume boundary.

Center of Mass

We must find some point for which the velocity is known and which could reasonably be taken to be a CM. Since the points p , e , and f all stride zone boundaries, the adjacent masses M_i depend upon the initially assigned zoning and can not in general be CM. Among our set of control points, only the zone center is a possible candidate. Depending upon the definition of M_i , there are two approaches to showing that the zone center is a CM. If the equal-mass definition of M_i is used, then the CM of a corner i can be defined to be

$$R_i = \begin{cases} \frac{1}{3}(x_p + x_z + x_e) & 2D \\ \frac{1}{4}(x_p + x_z + x_e + x_f) & 3D \end{cases} \quad 2.7.7$$

It can be shown that the above definitions for the auxiliary coordinates lead to

$$\begin{aligned} R_z &\equiv \frac{1}{M_z} \sum_i^z M_i R_i \\ &\rightarrow \frac{1}{M_z} \sum_i^z M_i x_p \\ &= x_z \end{aligned} \quad 2.7.8$$

so that the zone CM is indeed the auxiliary point x_z .

On the other hand, if one of the other definitions of M_i is used, then an approximate CM must be used for i . One such is defined

$$R_i \equiv \alpha x_p + (1 - \alpha) x_z \quad 2.7.9$$

where α varies between 0 and 1. Consider the substructure consisting of the set of corners which share points p and z . Although this definition is seemingly inappropriate for individual corners, it has the effect of setting the CM for this substructure on the line between p and z , a reasonably good approximation. Then, the CM for the zone again reduces to

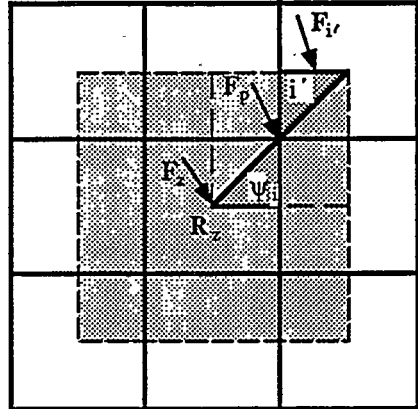


Figure 8. Extended and true zone control volumes.

$$\begin{aligned} R_z &\equiv \frac{1}{M_z} \sum_i^z M_i R_i \\ &= \frac{1}{M_z} \left\{ \alpha \sum_i^z M_i x_p + (1 - \alpha) x_z \sum_i^z M_i \right\} \\ &= x_z \end{aligned} \quad 2.7.10$$

Torque

For the momentum control volume, the forces F_i are applied at some position x_i on the surfaces S_i . The total force F_p on a point p and torque T_p about some point R are given by

$$\begin{aligned} F_p &= \sum_i^p F_i \\ T_p(R) + \tau_p &\equiv \sum_i^p x_i \times F_i \\ &= R \times \sum_i^p F_i + \sum_i^n (x_i - R) \times F_i \\ &= R \times F_i + \tau_p \end{aligned} \quad 2.7.11$$

Consider the extended zone control volume formed by the median mesh passing through the centers of adjacent zones as shown in Figure 8. The forces F_i are applied at the surface of the extended zone, but accelerate only the true zone. Define the mass fractions

$$\Psi_i \equiv M_i / M_p \quad 2.7.12$$

which are used to conservatively divide the point forces among the zones with which they interact.

$$\begin{aligned} F_z &\equiv \sum_i^z \psi_i F_p \\ &= \sum_i^z \psi_i \sum_{i'}^p F_{i'} \end{aligned} \quad 2.7.13$$

The notion of splitting the point forces in this manner requires some explanation. The point force produces a momentum change within the point control volume. Since all points within the volume have the same velocity, the momentum change is correctly apportioned to subvolumes according to the mass fractions.

Similarly, the torque applied to a node can be resolved into torques at and about the CM, and can be distributed to the zone by mass fraction. These resulting forms for torque correspond to the same control volumes used in the linear momentum equations.

$$\begin{aligned} T_z(R_z) + \tau_z &\equiv \sum_i^z \psi_i [T_p(R_z) + \tau_p] \\ &= \sum_i^z \psi_i \sum_{i'}^p \mathbf{x}_{i'} \times \mathbf{F}_{i'} \\ &= R_z \times \sum_i^z \psi_i \sum_{i'}^p \mathbf{F}_{i'} \\ &\quad + \sum_i^z \psi_i \sum_{i'}^p (\mathbf{x}_{i'} - R_z) \times \mathbf{F}_{i'} \\ &= R_z \times F_z + \tau_z \end{aligned} \quad 2.7.14$$

The equation for the zonal linear momentum is in nonlocal conservation form because the currents sum to zero at the extended zone boundary instead of the true zone boundary

$$\begin{aligned} M_z \dot{u}_z &= \sum_i^z M_i \dot{u}_p \\ &= \sum_i^z \psi_i M_p \dot{u}_p \\ &= \sum_i^z \psi_i F_p \\ &= F_z \end{aligned} \quad 2.7.15$$

The acceleration equations for the zone are of lower spatial order than those for the node. The conservation law for angular momentum at zone z is then proved

$$\begin{aligned} \dot{L}_z &\equiv M_z R_z \times \dot{u}_z \\ &= R_z \times M_z \dot{u}_z \\ &= R_z \times F_z \\ &= T_z \end{aligned} \quad 2.7.16$$

No similar law can be proved at the point because it is not a CM.

Although conservation of angular momentum on the global scale has never been in question, this work shows conservation on a scale somewhat larger than a zone. The lack of such conservation on the scale of momentum control volumes gives rise to numerical instabilities such as chevron and hourglass modes.

Conservation Law

The equation for the nodal momentum is in conservation form

$$M_p \dot{u}_p = F_p$$

3. CONCLUSIONS

Hydrodynamics algorithms are often formulated in a relatively *ad hoc* manner in which independent discretizations are proposed for mass, momentum, energy, and so forth. We have shown that, once discretizations for mass and momentum are stated, the remaining discretizations are very nearly uniquely determined, so there is very little latitude for variation. The resulting analysis provided some known results and several previously unreported surprises.

- As has been known (and largely ignored for some years) the kinetic energy discretization must follow directly from the momentum equation; and the internal energy must follow directly from the energy currents affecting the kinetic energy.
- Because energy is not exactly conserved in traditional PDV formulations of SGH, such formulations are not in principle reversible.
- Requirements for reversibility and thermodynamic consistency unexpectedly forces the replacement of the usual volume calculation with a conservation integral.
- Reversibility considerations further forbid the use of higher order functional representations for either velocity or stress within zones or control volumes, forcing the use of a constant stress element and a constant velocity control volume.
- In turn the constant stress model causes the zone center coordinates to formally disappear from the formulation. Likewise the constant velocity model causes the point coordinates to formally disappear from the Cartesian formulation, removing the direct need for hourglass corrections
- The form of the work equations and the requirement for dissipation by viscous forces

strongly limits the possible algebraic forms for artificial viscosity. We have proposed a distinction based upon the shock dissipation and numerical smoothing functions of artificial viscosity and have presented forms for both, as well as two spatial centerings of the viscosity tensor.

- The momentum equation and a center-of-mass definition lead directly to an angular momentum conservation law which is satisfied by the system. Although conservation of angular momentum on the global scale has never been in question, this work shows conservation on a scale somewhat larger than a zone. The lack of such conservation on the smaller scale of momentum control volumes gives rise to numerical instabilities such as chevron and hourglass modes.
- It was shown that, by a few straightforward substitutions, the Cartesian formulation can be converted to a multidimensional curvilinear one. The resulting equations for momentum and quantities derived from it are not in strict conservation form and some conservation error occurs near the axis.
- The formulation in 2D axisymmetric geometry was shown to preserve rotational symmetry.

Acknowledgments

The author wishes to acknowledge A. Harrison, D. Miller, D. Lappa, and T. Palmer for their collaboration and helpful criticisms on the manuscript. He further gratefully acknowledges D. Nielsen Jr., D. Nowak, the NWT Directorate, and the LDRD committee for their continuing support of the work. This work was performed under the auspices of the U.S. Department of Energy, by Lawrence Livermore National Laboratory under Contract #W-7405-Eng-48.

APPENDIX A CURVILINEAR GEOMETRY

This appendix presents, without proof, curvilinear formulations in 1D (Cartesian, spherical, and cylindrical) and 2D (Cartesian and axisymmetric). We will retain the form of the 3D expressions previously presented, but indicate the replacements that must be made to achieve the curvilinear form. The basic method involves replacement of the finite volume surface integrals with corresponding integrals of lower dimension (e.g., line integrals in 2D) and addition of geometrical $1/r$ terms that formally appear as sources.

The resulting equations for momentum and quantities derived from it are not in strict conservation form and some error occurs near the axis. Exact conservation could be assured by also including the error terms as sources, but exact rotational symmetry would be lost in 2D.

Rotational Symmetry

The 2D axisymmetric formulation presents a special problem, that of *rotational symmetry*. If a spherically symmetric flow field is calculated in 2D axisymmetric geometry using rotationally symmetric zoning, then an exactly symmetrical result should be obtained. If not, a numerical algorithm will be prone to generating spurious vorticity especially along the axis. Generally, we achieve rotational symmetry by replacing the finite volume surface integrals with line integrals and introducing geometrical terms in $1/r$. The resulting method is symmetrical, employs an energy-conserving formulation, and moreover avoids the unintended introduction of entropy by the difference equations. However, like other symmetrical formulations, the conservation equations are not in strict conservation form and errors occur near the axis.

A numerical algorithm can be tested for rotational symmetry by comparing the difference

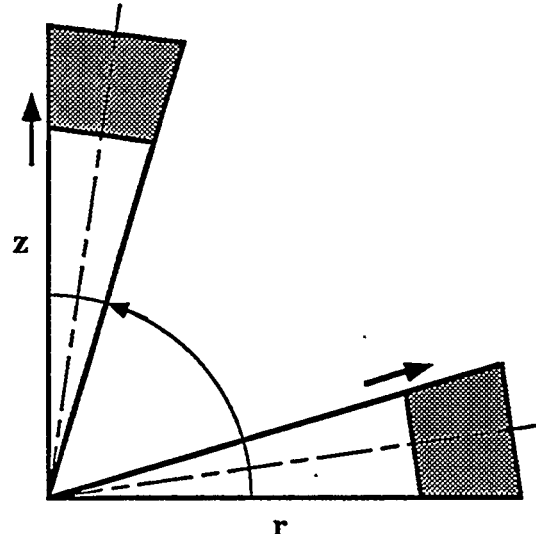


Figure A1. Thought experiment for rotational symmetry.

equations for a zone on the symmetry axis with another at some other angle (shown in Figure A1). This is a relatively difficult test to pass. The proof in most cases amounts to showing that the expressions in question rotate as

$$E = \frac{Ar_a}{Br_b} \rightarrow \frac{Ar_a \cos\theta}{Br_b \cos\theta} = E$$

in which both r_a and r_b correspond to points on the line from the origin through the zone center.

A.1 GEOMETRY

Define

$$\alpha = \begin{cases} 0 & \text{cartesian} \\ 1 & \text{cylindrical / axisymmetric} \\ 2 & \text{spherical} \end{cases}$$

A.1.1

Surface areas

Surface areas in the Cartesian formulation are replaced by

$$\begin{aligned} S_i &= s_i r_p^\alpha \\ T_i &= t_i r_p^\alpha \end{aligned} \quad \text{A.1.2}$$

where in 1D

$$\begin{aligned} s_s(1) &= \text{sgn}(x_{21}) \mathbf{i} \\ t_s(1) &= \text{sgn}(x_{21}) \mathbf{i} \\ s_i(1) &= \pm s_s \\ t_i(1) &= \pm t_s \end{aligned} \quad \text{A.1.3a}$$

and in 2D

$$\begin{aligned} s_s(2) &= \mathbf{k} \times (\mathbf{x}_e \times \mathbf{x}_z) \\ t_s(2) &= \mathbf{k} \times (\mathbf{x}_1 \times \mathbf{x}_2) \\ s_i(2) &= \pm s_s \\ t_i(2) &= t_s/2 \end{aligned} \quad \text{A.1.3b}$$

where \mathbf{i} and \mathbf{k} are respectively unit vectors in the r and out-of-plane directions.

Volume

Volume conservation in the curvilinear formulation is exact but, as in the Cartesian form, not a direct function of coordinates. However, the *initial* areas and volumes are defined by coordinate areas and volumes A_i and B_i of corners

$$\begin{aligned} a_z^{00} &= \sum_i^z A_i(\mathbf{x}_p, \mathbf{x}_z, \mathbf{x}_e, \mathbf{x}_f) \\ V_z^{00} &= \sum_i^z B_i(\mathbf{x}_p, \mathbf{x}_z, \mathbf{x}_e, \mathbf{x}_f) \end{aligned} \quad \text{A.1.4}$$

Specifically,

$$A_i = \frac{1}{2} \begin{cases} |\mathbf{x}_{21}| & 1D \\ (\mathbf{x}_{21} \times \mathbf{x}_{z1})/2 & 2D \\ V_s^{00} & 3D \end{cases} \quad \text{A.1.5}$$

and B_i is the corresponding volume of revolution. At each timestep, the zone area and volume change is calculated from the conservative integrals

$$\begin{aligned} \delta a_z &= \delta t \sum_i^z t_i \cdot \mathbf{u}_p \\ \delta V_z &= \delta t \sum_i^z r_p^\alpha t_i \cdot \mathbf{u}_p \end{aligned} \quad \text{A.1.6a}$$

This discretization of δV is consistent with the work equation. A commonly used alternative

$$\delta V_z = \delta t r_z \left[\sum_i^z t_i \cdot \mathbf{u}_p + \frac{\alpha}{r_z} \sum_i^z a_i \mathbf{u}_p \right] \quad \text{A.1.6b}$$

is not. The accumulated area and volumes are then

$$\begin{aligned} a_z &= a_z^{00} + \sum_t \delta a_z \\ V_z &= V_z^{00} + \sum_t \delta V_z \end{aligned} \quad \text{A.1.7}$$

We have omitted multiplicative factors involving π . The mass fractions ϕ_i are constants determined as before and are used to define

$$a_i = \phi_i a_z \quad \text{A.1.8}$$

In 2D axisymmetric geometry, ratios like $\delta V_z / V_z^{00}$ do have rotational symmetry. For spherical flow, the expressions for both δV_z and V_z can be shown to be composed of terms effectively evaluated on the line from the origin through the zone center, so that the ratio is rotationally symmetric.

A.2 MASS

In curvilinear geometry, zone and point masses are defined in distinctly different manners. Zone mass is used principally in determining density for EOS calculations and is defined

$$\begin{aligned} M_z &= \rho_z^{00} V_z^{00} \\ &= \text{constant} \\ \rho_z &\equiv \frac{M_z}{V_z} \end{aligned} \quad \text{A.2.1}$$

In order to produce a rotationally symmetric momentum equation in 2D, point mass is defined in terms of an areal quantity

$$m_z = \rho_z a_z \quad A.2.2$$

and is not exactly conserved. The quantity m_z is partitioned according to mass fraction φ_i

$$\begin{aligned} m_i &= \varphi_i m_z \\ m_p &= \sum_i^p m_i \\ M_p &= m_p r_p^\alpha \\ &\neq \text{constant} \end{aligned} \quad A.2.3$$

The point masses M_p are not constant because r_p is not exactly the CM of the momentum control volume. However, large errors should only occur near $r_p=0$.

A.3 MOMENTUM CONSERVATION

Forces

For brevity, we combine the reversible and irreversible stress tensors into a single σ_i . The forces F_i centered on the surfaces S_i are

$$F_i = (f_i + g_i) r_p^\alpha \quad A.3.1$$

The expression for F_p is unchanged from the Cartesian form. The necessary equations for f and g follow from the differential expressions for the divergence operator and are given by

$$\begin{aligned} f_i &= S_i \cdot \sigma_i \\ g_i &= \frac{a_i}{r_z} \begin{cases} 2(\sigma_{rr} - P) & \text{1D cylindrical} \\ 3(\sigma_{rr} - P) & \text{1D spherical} \\ \begin{bmatrix} \sigma_{rr} - \sigma_{\varphi\varphi} \\ \sigma_{rz} \end{bmatrix} & \text{2D axisymmetric} \\ 0 & \text{otherwise} \end{cases} \end{aligned} \quad A.3.2$$

Because the surface areas satisfy

$$S_{i_1} = -S_{i_2} \quad A.3.3$$

the finite volume formulation produces f forces that sum to zero on the boundary of the momentum control volume; that is,

$$f_{i_1} = -f_{i_2} \quad A.3.4$$

The g forces arising from the curvilinear geometry appear as body forces.

Acceleration, Velocity, Coordinates

After the indicated substitutions the curvilinear form of the momentum equation is

$$m_p \dot{u}_p = \sum_i^p (f_i + g_i) \quad A.3.5$$

The velocity and coordinate integrations are unchanged. *Unlike the Cartesian formulation in which the point coordinate x_p drops out of the discretized equations, its component r_p appears repeatedly in the curvilinear formulation.*

We need to show that this momentum equation preserves rotational symmetry in the case of 2D axisymmetric geometry. Consider the element of area shown at two different orientations in the Figure A2. For a configuration with spherical symmetry, the stress tensor for the element on the r -axis will be given by

$$\begin{aligned} \sigma_{rr} &= \sigma_1 \\ \sigma_{zz} &= \sigma_2 = \sigma_3 = \sigma_{\varphi\varphi} \\ \sigma_{rz} &= \sigma_{12} = 0 \end{aligned} \quad A.3.6$$

The f forces depend only upon planar quantities and are clearly rotationally symmetric. However, the $1/r$ terms require explanation. Consider

$$\begin{aligned} a_r &\equiv \frac{\sigma_{rr} - \sigma_{\varphi\varphi}}{r} = \frac{\sigma_1 - \sigma_3}{r} \\ a_z &\equiv \frac{S_{rz}}{r} = \frac{\sigma_{rz}}{r} = \frac{\sigma_{12}}{r} = 0 \end{aligned} \quad A.3.7$$

We need to show that

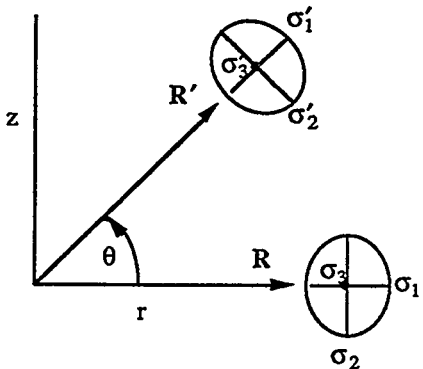


Figure A2. Rotational symmetry of g forces.

$$\begin{aligned} a'_r &= a_r \cos \theta - a_z \sin \theta = a_r \cos \theta \\ a'_z &= a_r \sin \theta + a_z \cos \theta = a_r \sin \theta \end{aligned} \quad A.3.8$$

In the rotated frame, the transformed quantities are

$$\begin{aligned} \sigma'_{rr} &= \sigma_1 \cos^2 \theta + \sigma_2 \sin^2 \theta \\ \sigma'_{zz} &= \sigma_1 \sin^2 \theta + \sigma_2 \cos^2 \theta \\ \sigma'_{rz} &= -(\sigma_2 - \sigma_1) \sin \theta \cos \theta \\ \sigma'_{\varphi\varphi} &= \sigma_3 \\ r' &= r \cos \theta \end{aligned} \quad A.3.9$$

For the postulated spherical flow conditions, $\sigma_3 = \sigma_2$, and it follows that spherical symmetry is indeed preserved

$$\begin{aligned} a'_r &\equiv \frac{\sigma'_{rr} - \sigma'_{\varphi\varphi}}{r'} \\ &= \frac{\sigma_1 \cos^2 \theta + \sigma_3 (\sin^2 \theta - 1)}{r \cos \theta} \\ &= \frac{(\sigma_1 - \sigma_3)}{r} \cos \theta \\ a'_z &\equiv \frac{\sigma'_{zz}}{r'} \\ &= \frac{(\sigma_1 - \sigma_2) \sin \theta \cos \theta}{r \cos \theta} \\ &= \frac{(\sigma_1 - \sigma_3)}{r} \sin \theta \end{aligned} \quad A.3.10$$

$$\begin{aligned} J_i &\equiv \delta t \mathbf{F}_i \cdot \mathbf{u}_p \\ &\rightarrow \delta t r_p^\alpha (\mathbf{f}_i + \mathbf{g}_i) \cdot \mathbf{u}_p \end{aligned} \quad A.4.1$$

$$\begin{aligned} W_z &= \sum_i^z J_i \\ &= \delta t \sum_i^z r_p^\alpha (\mathbf{f}_i + \mathbf{g}_i) \cdot \mathbf{u}_p \end{aligned} \quad A.4.2$$

Because the point mass is not exactly constant, some error is present in the kinetic energy, and consequently in the resulting current, work, and internal energy expressions. The radius in these expressions is evaluated at +.

A.4 ENERGY

The kinetic energy and energy current expressions are unchanged aside from the indicated substitutions which result in

APPENDIX B SAMPLE CALCULATIONS

The following are representative results for the hydrodynamics algorithm described. Although the 3D hydrodynamics algorithms are fully functional, we have yet to define non-trivial 3D test problems, so that no 3D results are presented. Because optimal settings for artificial viscosity are currently being investigated, the problems were run with different viscosity formulations as noted.

Notes

1 sh = 1.e-8 sec

1 jk = 1.e16 erg

B.1 1D SPHERICAL NOH PROBLEM

Geometry

1D spherical geometry

Sphere of radius 10 cm.

Zoning

100 equally spaced zones

Materials

Gamma law gas with $\gamma = 5/3$

Initial conditions

Density = 1.0 gm/cm³

Specific energy = 2.e-7 jk/gm

Velocity = 1 cm/sh toward origin except for origin itself which has velocity = 0

Boundary conditions

Origin is fixed

Outer radius is constant inward velocity of 1 cm/sh

Stop time

6 sh

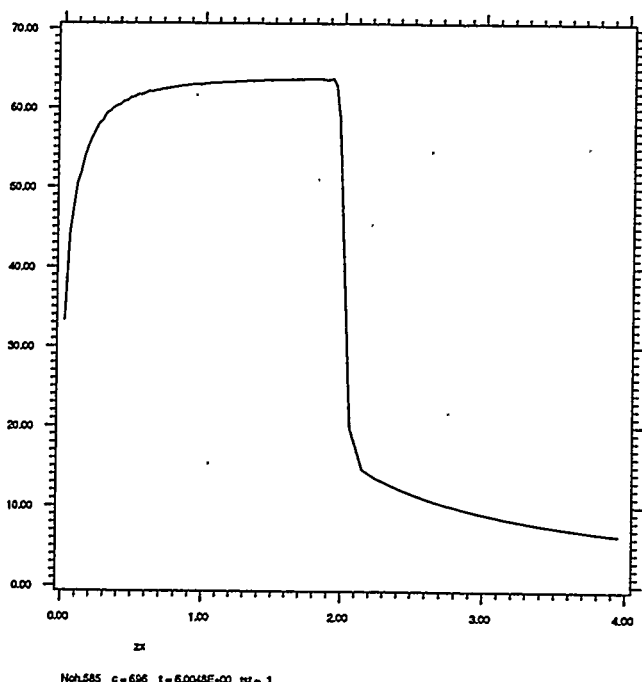


Figure B1.1 Density versus distance to zone centers. Exact result is a density of 64 behind the shock which extends to a radius of 2 cm.

B.2 2D THREE K-LINE NOH PROBLEM

Run with shock viscosity only (Equation 2.6.3, $q_1=1$, $q_2=1.33$). No hourglass, or other smoothing viscosity was used.

Geometry

2D axial geometry

Half sphere with origin at (0,0) and radius 1 cm.

Zoning

3 equally spaced radial (K) lines (0° , 45° , 90°)
200 equally spaced lateral (L) lines.

Materials

Gamma law gas with $\gamma = 5/3$

Initial conditions

Density = 1.0 gm/cm³
Specific energy = 2.e-7 jk/gm
Velocity = 1 cm/sh toward origin except for
origin itself which has velocity = 0

Boundary conditions

Radial line at 0° is z-fixed
Radial line at 90° is r-fixed
Origin is fixed
Outer radius is constant inward velocity of 1
cm/sh

Stop time

0.6 sh

Comment

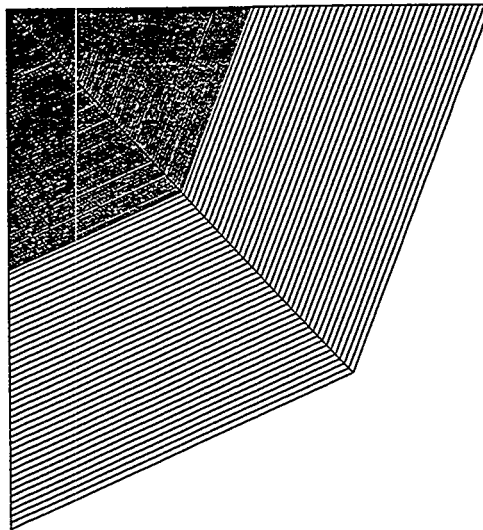


Figure B2.2 3KL Noh grid at stop time. Entire mesh. Apparent irregularities are due to graphical raster spacing, not the calculation itself.

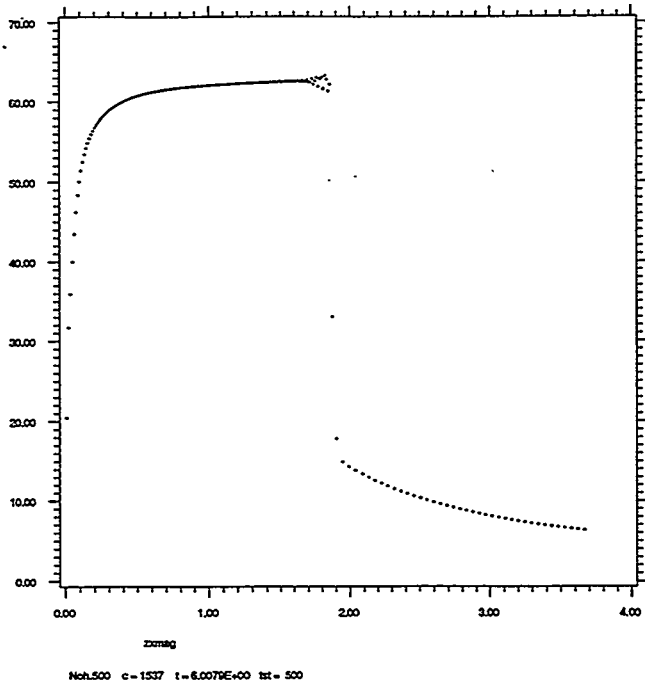


Figure B2.1 Density versus distance to zone centers. Exact result is a density of 64 behind the shock. If plotted versus point centers, the shock would extend to a radius of 2 cm.

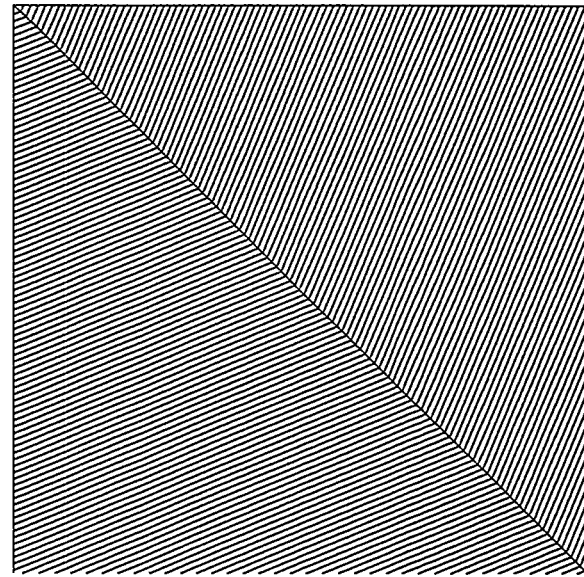


Figure B2.3 3KL Noh grid at stop time. Shock region. Apparent irregularities are due to graphical raster spacing, not the calculation itself.

B.3 SCHULZ ELLIPSE

Geometry

2D axial geometry

Half ellipse with radial semi-axis=18 cm, axial semi-axis=12 cm

Zoning:

10 equally spaced radial K lines extending from origin (0, 0) to the edge of the ellipse at angles from 0 to 90 in 10 degree increments. The innermost lateral L-line is the origin (0, 0). The next L-line is an ellipse with a radial semi-axis of 6 cm and a axial semi-axis of 4 cm. The remaining lateral L-lines are equally spaced from there to the edge of the ellipse.

Materials:

Gamma law gas with $\gamma = 5/3$

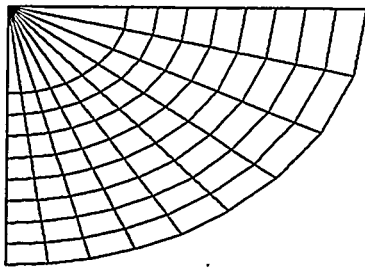


Figure B3.1 Schulz grid at 0.

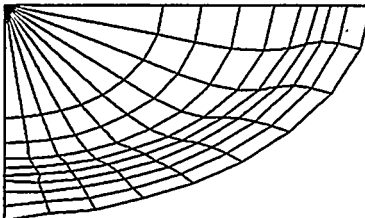


Figure B3.2 Schulz grid at 25.

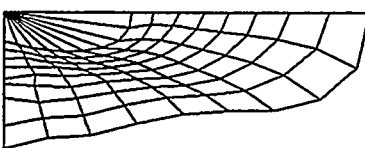


Figure B3.3 Schulz grid at 50.

Initial Conditions

Density = 1.845 gm/cm³

Specific energy = 2.e-7 jk/gm

Boundary Conditions

Vertical radial line is z-fixed

Pressure profile outside the ellipse that ramps from 0 jk/cm³ at t=0 to 0.1 jk/cm³ at t=5 sh and remains constant thereafter

Stop Time

100 sh

Comment

Run with a combination of shock viscosity (Equation 2.6.3, $q_1=1$, $q_2=1.33$) and smoothing viscosities (Equation 2.6.14, $q_v=q_d=q_w=0.5$)

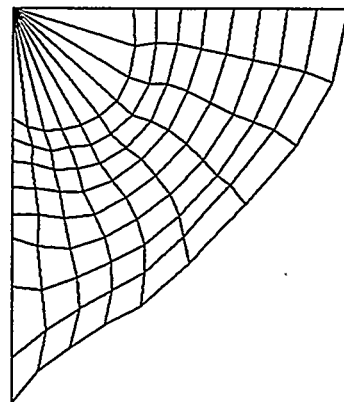


Figure B3.4 Schulz grid at 75.

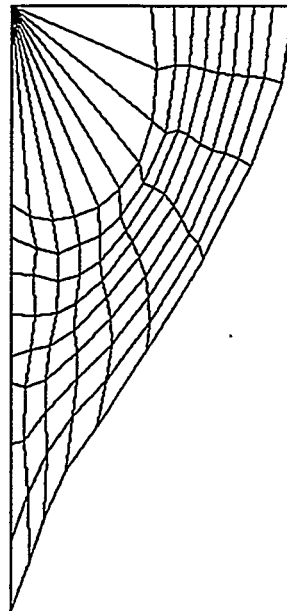


Figure B3.5 Schulz grid at 100.

B.4 SALTZMAN PROBLEM

Geometry

2D axial geometry

Cylinder of radius 0.1 cm and length 1.0 cm

Zoning:

For $K = 1$ to 101, $L = 1$ to 11,

$$z(K, L) = 0.01(L - 1) \sin\left[\frac{\pi(K - 1)}{100}\right] + 0.01(K - 1)$$

$$r(K, L) = 0.1 - 0.01(L - 1)$$

Materials

Gamma law gas with $\gamma = 5/3$

Initial conditions

Density = 1.0 gm/cm³

Specific energy = 2.e-7 jk/gm

Velocity = 0 except on boundary

Boundary Conditions

At $z=0$, velocity = 1 cm/sh directed toward
opposite end of cylinder

Boundaries at $r=0$ and $r=.1$ are both r-fixed

Boundary at $z=1$ is fixed

Stop Time

1 sh

Comment

Run with a side centered viscosities (Equation 2.6.13, $q_1=1$, $q_2=1.33$, $q_v=q_d=1$, $q_w=0$) and (Equation 2.6.14, $q_v=q_d=0$, $q_w=.5$)

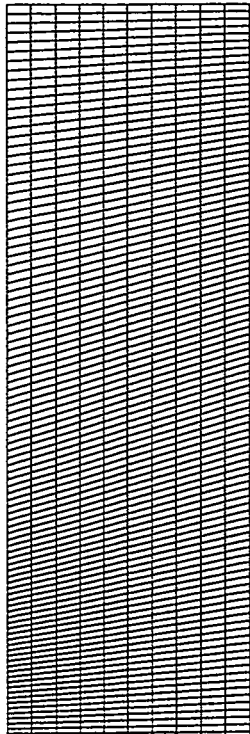


Figure B4.1 Saltzman grid at 0.0, expanded in the radial direction.

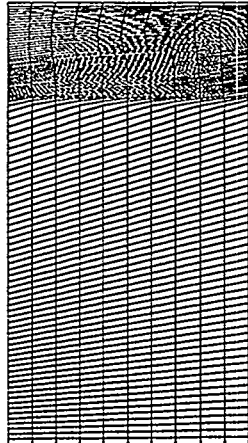


Figure B4.2 Saltzman grid at 0.4, expanded in the radial direction.



Figure B4.3 Saltzman grid at 0.8, expanded in the radial direction.

REFERENCES

- 1 A.A. Amsden and C.W. Hirt, "YAQUI: An Arbitrary Lagrangian-Eulerian Computer Program for Fluid Flow at All Speeds," Los Alamos National Laboratory, Report LA-5100, 1973.
- 2 W.P. Crowley, "FLAG: A Free-Lagrange Method for Numerically Simulating Hydrodynamic Flows in Two Dimensions," *Proceedings of the Second International Conference on Numerical Methods in Fluid Dynamics*, (Springer-Verlag, New York, 1970), pp. 37-43.
- 3 J.R. Pasta and S. Ulam, "Heuristic numerical work in some problems of hydrodynamics," in *Math. Tables and other Aids to Computation*, 1959, vol XIII, N 65, p. 1-12.
- 4 J.P. Boris, M. Fritts, and K.L. Hain, "Free Surface Hydrodynamics Using a Lagrangian Triangular Mesh," *Proc. First Inter. Conf. on Numerical Ship Hydrodynamics*, Gaithersburg, MD, October 1975.
- 5 M.J. Fritts and J.P. Boris, "The Lagrangian Solution of Transient Problems in Hydrodynamics Using a Triangular Mesh," *J. Comp. Phys.*, 31, 173 (1979).
- 6 V.F. D'yachenko, "Some new methods for numerically solving nonstationary gas dynamics problems," *USSR Computational Mathematics and Mathematical Physics*, 1965, vol. 5, no. 4, pp. 680-688.
- 7 F.L. Addressio, M. Cline, and J.K. Dukowicz, "A General Topology Godunov Method," in *Particle Methods in Fluid Dynamics and Plasma Physics* (North-Holland, Amsterdam, 1988, J.U. Brackbill and J.J. Monaghan, editors).
- 8 W.P. Crowley, "Free-Lagrange Methods for Compressible Hydrodynamics in Two Space Dimensions," in *The Free Lagrange Method* (Springer-Verlag, New York, 1985, M.J. Fritts, W.P. Crowley, and H. Trease, editors).
- 9 J. von Neumann and R. Richtmyer, "A Method for the Numerical Calculation of Hydrodynamic Shocks," *J. Appl. Phys.* 21, 232 (1950).
- 10 O.C. Zienkiewicz, *The Finite Element Method in Engineering Science* (McGraw-Hill, New York, 1971).
- 11 W.D. Schulz, "Two-Dimensional Lagrangian Hydrodynamic Difference Equations," in *Methods of Computational Physics, Vol. 3* (Academic Press, New York, 1964, B. Alder, S. Fernback, and M. Rotenberg, eds.).
- 12 D.E. Burton, "Connectivity Structures and Differencing Techniques for Staggered-Grid Free-Lagrange Hydrodynamics," IMACS PDE7 Conference, Rutgers University, June 1992. Lawrence Livermore National Laboratory Report, UCRL-JC-110555, June 1992.
- 13 D.E. Burton, "Exact Conservation of Energy and Momentum in Staggered-Grid Hydrodynamics with Arbitrary Connectivity," in *Advances in the Free Lagrange Method* (Springer Verlag, NY 1990). Lawrence Livermore National Laboratory Report UCRL-JC-104258, June 1990.
- 14 D.E. Burton, "Conservation of Energy, Momentum, and Angular Momentum in Lagrangian Staggered-Grid Hydrodynamics," Lawrence Livermore National Laboratory Report UCRL-JC-105926, November 1990.

¹⁵ R.E. Cooper, "Data Structures and Vectorization in a Two-Dimensional Free-Lagrangian Code," in *The Free Lagrange Method* (Springer-Verlag, New York, 1985, M.J. Fritts, W.P. Crowley, and H. Trease, editors).

¹⁶ J.G. Trulio and K.R. Trigger, "Numerical Solution of the One-Dimensional Lagrangian Hydrodynamic Equations," Lawrence Livermore National Laboratory, Report UCRL-6267, 1961.

J.G. Trulio and K.R. Trigger, "Numerical Solution of the One-Dimensional Hydrodynamic Equations in an Arbitrary Time-Dependent Coordinate System," Lawrence Livermore National Laboratory, Report UCRL-6522, 1961.

¹⁷ P.L. Browne and K.B. Wallick, "Reduction of Mesh Tangling in Two-Dimensional Lagrangian Hydrodynamics Codes by the Use of Viscosity, Artificial Viscosity, and TTS (Temporary Triangular Subzoning for Long Thin Zones)," Los Alamos Scientific Laboratory Report, LA-4720-MS, November 1971.

¹⁸ G. Maenchen and S. Sack, "The TENSOR Code," in *Methods of Computational Physics, Vol. 3*, Academic Press, New York, 1964.

¹⁹ L.G. Margolin and B.D. Nichols, "Momentum Control Volumes for Finite Difference Codes," Third International Conference on Numerical Methods in Laminar and Turbulent Flow, Seattle, August 1983. Los Alamos National Laboratory Report LA-UR-83-524.

²⁰ M.L. Wilkins, "The Use of Artificial Viscosity in Multidimensional Fluid Dynamic Calculations," *Jour. Comp. Phys.*, 36, p. 281 (1990).

V.F. Kuropatenko, "On Difference Methods for the Equations of Hydrodynamics," in *Difference Methods for Solutions of Problems of Mathematical Physics I* (N.N. Janenko, ed.), p. 116, American Mathematical Society, Providence, RI, 1967.

²¹ R. Barton, as discussed by L.G. Margolin "A Centered Artificial Viscosity for Cells with Large Aspect Ratios," Lawrence Livermore National Laboratory Report UCRL-53882, August 1988.